Prediction of Performance of MSE Embankment Using Steel Grids on Soft Bangkok Clay

D.T. Bergado — Associate Professor, Asian Institute of Technology, Bangkok, Thailand
Jin-Chun Chai — Research Engineer, Asian Institute of Technology, Bangkok, Thailand
A.S. Balasubramaniam — Professor, Asian Institute of Technology, Bangkok, Thailand

ABSTRACT: The behavior of a full scale test reinforced wall/embankment on Bangkok clay has been predicted by finite element method. In the numerical modelling, two aspects have been emphasized: (1) selecting proper soil/reinforcement interface properties according to the relative displacement pattern (direct shear or pullout) of upper and lower interface elements between soil and reinforcement; and (2) simulating the actual construction process by updating the node coordinates including those of the wall or embankment elements above the current construction level which ensures that the applied fill thickness simulate the actual field value. Finite element results were compared with the field data in terms of excess pore pressures, settlements, lateral displacements, tension forces in the reinforcements, and base pressures. It was found that the foundation settlements and the wall face lateral displacement were predicted reasonably well. In addition, the predicted pore pressures, tension forces in reinforcements, foundation lateral displacements, and embankment base pressures agreed fairly with measured values. Several influence factors, such as permeability variation of the foundation soil and compaction effects of embankment fill have also been investigated. Furthermore, some of the difficiencies in finite element modelling are also discussed.

INTRODUCTION

For the last two decades, extensive researches and investigations have been carried out to understand the behavior and mechanisms of the reinforced earth structures. The behavior of the reinforced walls and embankments on soft ground have been analyzed by several investigators using finite element methods (e.g. Hird and Pyrah, 1990; Adib et al, 1990). However, the accuracy of the finite element analysis mainly depends on the accuracy of the models used and the correctness of the parameters inputted into the models. Although different soil models, such as nonlinear hyperbolic and modified Cam clay, have been used to represent the stress/strain behavior of the soils, the soil/reinforcement interface properties and actual construction process are not properly simulated. All these factors influence the ability of using finite element method to predict the behavior of reinforced wall/embankment on soft ground.

The most important parameters controlling the performance of the reinforced earth structure, among others, are the soil/reinforcement interface properties. The interface properties are usually determined by direct shear or pullout tests. However, for grid reinforcements, the different soil/reinforcement interaction modes (direct shear or pullout) yields different interface properties. In order to properly simulate the soil/reinforcement interaction behavior, it should be considered in the numerical modelling to use different properties for different interaction mode (Rowe and Mylleville, 1988).

In finite element analysis, the wall or embankment load is applied by one of the following methods: (1) by increasing of the gravity of the whole or part of wall or embankment elements; and (2) by placing a new layer of wall or embankment elements. For the case of embankment construction, if the incremental load is applied by increasing the gravity of the whole embankment, in the beginning, the center part of the embankment is loaded more, while the area near the toe is loaded less than the actual value. Furthermore, the stiffness of the embankment may not be modelled properly. However, if the incremental load is applied by applying a new layer of elements, the node coordinates of the embankment elements above the current construction level must be updated to account for the deformation during the construction process. Otherwise, the applied total fill thickness will be more than the actual value especially in the case of embankment on soft ground. Most computer programs used for analyzing the behavior of embankment on soft ground do not treat this factor well. The original CRISP program (Britto and Gunn, 1987) did not consider this factor, and the CESAR program (Magnan and Kattan, 1989) assumed that the mechanical properties of the embankment fill elements exist from the beginning even when the element gravity load is not applied.

In this paper, the concepts of considering the different soil/reinforcement interaction modes and simulating the actual construction process are presented first. A full scale test reinforced embankment is then analyzed by the proposed finite element method. Consequently, the finite element results are compared with the field data. Finally, some of the difficulties in finite element modeling are discussed.

NUMERICAL MODELLING

General Aspects

The reinforced wall/embankment on soft ground system has been modelled by finite element method under plane strain condition. All the elements are formulated as isoparameteric elements. Discrete material approach is used to model the reinforced wall/embankment on soft ground system so that the properties and responses of the soil/reinforcement interaction can be directly quantified. The face panel of reinforced wall is modelled by 3-node beam elements with axial, shear and bending stiffness. The reinforcement is modelled by 3-node bar elements. The soil/reinforcement and soil/wall face interfaces are modelled by 6-node zero thickness joint elements. The soil elements are modelled by 8 or 6-node solid elements with or without pore pressure degree of freedoms. Finally, nodal links are used at the free end of reinforcement to allow realistic vertical stress condition (Collin, 1986).

Several soil behavior models are employed in the analysis. The behavior of the soft foundation soil is controlled by modified Camclay model (Roscoe and Burland, 1968). The linear elastic/perfect plastic model is used to model the heavily overconsolidated clay, and the yielding is controlled by Mohr-Coulomb criterion. The backfill soil is modelled by hyperbolic constitutive model (Duncan et al, 1980). The

compaction operation is modelled by bi-linear hysteretic loading/unloading model (Duncan and Seed, 1986). The consolidation process of soft ground is simulated by coupled consolidation theory (Biot, 1941).

In modelling the soil/reinforcement interface behavior, two interaction modes are considered, namely: pullout and direct shear modes. The hyperbolic shear stress/shear displacement model (Clough and Duncan, 1971) is used to represent direct shear interaction mode. Pullout resistance of grid reinforcement consists of skin friction in the longitudinal members and bearing resistance in the transverse members. The skin friction is modelled by linear elastic-perfect plastic model and the pullout bearing resistance is simulated by a hyperbolic bearing resistance model which is only valid for grid reinforcements (Chai, 1992). The techniques of selecting proper interface properties and simulating the actual construction procedure are briefly discussed below.

Modelling Different Soil/Reinforcement Interaction Modes

Soil/reinforcement interaction mode can either be direct shear or pullout. For grid reinforcement, these two different interaction modes will yield different interface strength and deformation parameters. The interface elements above and below reinforcement work as pair elements and the direct shear (the same sign of shear stresses) and pullout (different sign of shear stresses) soil/reinforcement interaction modes are automatically adopted according to their relative shear displacement pattern.

Pullout of reinforcement especially the grid reinforcement from the soil is a truly three-dimensional problem and it can only be approximately modelled in a two-dimensional analysis. It is assumed that the pullout resistance is uniformly distributed over the entire interface areas. Pullout interface shear stiffness consists of stiffness from skin friction resistance, k_{sf}, stiffness from passive bearing resistance, k_{sp}, respectively. The total equivalent tangential shear stiffness k_s is the sum of k_{sf} and k_{sp}.

$$k_s = k_{sf} + k_{sp} \tag{1}$$

For both direct shear and pullout interaction modes, when the normal stress at the interface is in tension, a very small (e.g. 100 kN/m^3) normal and shear stiffness are assigned to allow the opening and slippage at interface.

Simulating the Actual Construction Process

The actual embankment construction is carried out by placing and compacting the fill material layer by layer. Therefore, in finite element analysis, the incremental load should be applied by placement of embankment elements one layer after another. In analyzing the problems, such as embankment on soft ground, the large deformation

phenomenon can be considered by updating the node coordinates during the incremental analysis. In this case where considerable deformation occurs during the construction process, the coordinates of the wall or embankment elements above current construction level are also corrected based on the following assumptions: (a) the original vertical lines are kept at vertical direction, and the horizontal lines remained straight; (b) the incremental displacements of the nodes above current construction top surface are linearly interpolated from the displacements of the two end nodes of current construction top surface according to their x-coordinates (horizontal direction). This operation ensures that the applied fill thickness is the same as the actual value and, thus, the actual construction process is most closely simulated.

TEST REINFORCED EMBANKMENT AND INPUT PARAMETERS

Test Reinforced Embankment

The full scale welded steel grid reinforced test embankment was constructed on the campus of Asian Institute of Technology (AIT). The original embankment was 5.8 m (19.5 feet) above the existing ground surface with about 26.0 m (87 feet) base length. It has three sloping faces with 1:1 slope and one vertical front face (wall). The welded wire mats used in the test wall/embankment system consisted of W4.5(6.1mm) x W3.5(5.4mm) galvanized welded steel wire mesh with 152mm x 228mm (6x9 inches) grid openings in the longitudinal and transverse directions, respectively. The length of reinforcement was 5 m and the vertical spacing between the reinforcements was 0.45 m. The cross-sectional view of the embankment is shown in Fig. 1a, b. The subsoil profile at the site consists of the topmost 2.0 m thick layer of dark-brown weathered clay overlying a blackish-grey soft clay layer which extends to a depth of about 8 m below the existing ground. The soft clay layer is underlain by a stiff clay layer. A typical subsoil profile together with the general soil properties at this site is depicted in Fig. 2. The finite element mesh and the boundary conditions are shown in Fig. 3. The bar and beam elements are indicated by darker solid line. For clarity, the interface elements are not shown in the mesh. The horizontal boundaries were selected far enough from the reinforced embankment, so as to have negligible influence on the structure response. The vertical fixed boundary was selected at 12 m depth because as can be seen in Fig. 2 at this depth, the subsoil is very stiff.

Model Parameters

The linear elastic-perfectly plastic model parameters for topmost 1.0 m thick weathered clay layer and modified Camclay parameters for soft to medium stiff clay layers are shown in Table 1. The parameters were determined based on actual test data (Balasubramaniam et al, 1978; Asakami, 1989) and some of them are shown in Fig. 4. Since there is uncertainty of the permeability of the foundation soil, 3 sets of permeabilities, namely: high, middle, and low permeabilities, were determined based on existing information (Ahmed, 1977; Bergado, 1990) and indicated also in Table

1. The top 2 m weathered clay is overconsolidated with an average overconsolidation ratio (OCR) of 5 and the underlying soil layers are slightly overconsolidated with an average OCR of 1.2.

The hyperbolic, non-linear elastic soil model parameters for compacted lateritic fill material (middle section of the embankment) are tabulated in Table 2, which were determined based on triaxial unconsolidated undrained (UU) test results (Bergado et al, 1988) and followed the technique established by Duncan et al (1980).

The interface hyperbolic direct shear model parameters were determined from direct shear test results of the fill material (Macatol, 1990). The adopted parameters were: friction angle, ϕ, of 32.5 degrees, cohesion, C, of 60 kPa, shear stiffness number, k_1, of 10500, shear stiffness exponent, n_1, of 0.72, and failure ratio, R_{f1}, of 0.85. The skin friction parameters between reinforcement frictional surface and lateritic soil were determined from test results of Shivashankar (1991) with adhesion of 50 kPa, skin friction angle of 9 degrees. The spacing between the grid reinforcement bearing member was 225 mm and the diameter of the bearing member was 5.4 mm. For both direct shear and pullout models, the normal stiffness of the interface was defined as 10^7 kN/m^3 for compression case and 10^2 kN/m^3 for tension case.

For welded wire reinforcement including the wall face, the Young's modulus was $2.0 \cdot 10^8$ kPa and the cross-sectional area of longitudinal bar per meter width was 180 mm^2. For the reinforcement, the yielding stress was $6.0 \cdot 10^5$. For the wall face, the shear modulus was $8.3 \cdot 10^7$ kPa, and the moment of inertia of cross sectional area was 45 mm^4 which was the sum of the moment of inertia of individual bars within 1.0 m width. The shear and normal stiffness for nodal link were assigned as $1.5 \cdot 10^4$ kN/m and $5.0 \cdot 10^6$ kN/m, respectively, for the current problem.

The parameters adopted for hysteretic compaction model (Duncan and Seed, 1986) were: at-rest lateral earth pressure coefficient, k_o, of 0.55, friction component of limiting coefficient of at-rest lateral earth pressure, $k_{1,\phi}$, of 2.21, cohesion under dynamic load, C_d, of 50 kPa, at-rest lateral earth pressure coefficient for unloading and reloading, k_2, of 0.15, and softening depth of 0.4 m. Considering light compactor (i.e. Ingersollrand, D 23) and the factor that there was about 0.3 m gap between wall face and the soil being compacted which was later filled up during the placement of next reinforcement layer, the peak compaction induced lateral stress profiles used in the analysis are shown in Fig. 5. The effect of the compaction operation on soft ground soil was ignored.

Finite Element Analysis

The wall/embankment above the ground surface was simulated by 13 incremental layers. For each layer, the gravity force was applied by two increments. Totally 6 analyses have been conducted. The first three of analyses were using 3 sets of the permeabilities listed in Table 1, respectively. Analysis number 4 used middle permeability but with compaction effect. Both analyses numbers 5 and 6 were conducted with two different options of varying the permeability during the loading and consolidation process. For analysis number 5 (varied I), the permeability was varied with the formula proposed by Taylor (1948) and verified by the Tavenas et al (1983) as follows:

$$k = k_o 10^{[-(e_o - e)/c_k]} \tag{2}$$

where e_o is the initial void ratio; e is the void ratio at the condition under consideration; k is the permeability; k_o is the initial permeability; and c_k is constant, which is equal to 0.5 e_o (Tavenas et al, 1983). The initial value of permeability was the middle permeability.

For analysis number 6 (varied II), the permeability variation was also controlled by Eq. 2. However, the values of permeability of the soft soil were different before and after yield with much higher value before yield (Tavenas and Leroueil, 1980). In this analysis, before the soil yield (yielding is controlled by modified Camclay model), the high permeability values (Table 1) were used and after the soil yielded, the permeability values of 1/5 of the values before the yield were adopted, i.e. low permeability in Table 1. A computer program named CRISP-AIT which was developed by modifying the CRISP computer program (Britto and Gunn, 1987), was used for the analyses. All the analyses were consolidation analyses.

PREDICTED RESULTS AND COMPARISON WITH FIELD DATA

Since the prediction is class C type prediction (Lambe, 1973), the predicted results are presented together with the field data. The data included excess pore pressures, vertical settlements, wall face and subsoil lateral displacements, tension forces in the reinforcements, and the wall/embankment base pressures. The finite element results obtained by using middle permeability with compaction effect that are mainly used as predicted values. The results of using high and low permeabilities (Table 1) did not predict the field data well. For the sake of clarity they are omitted from the presentation. However, some of the results from varied permeability analyses and using the middle permeability without compaction effect are also included for discussion.

Excess Pore Pressures

For predicting the excess pore pressure, the key parameter is the permeability of the subsoil. Figures 6 and 7 show the typical predicted excess pore pressure variations with different assumptions of the foundation permeability together with the field data at piezometer points 4 m and 7 m below the ground surface. The agreement between predicted and measured data is fairly good. From the figures, it can be seen that all the analyses overpredicted the excess pore pressure at the end of construction. However, the varied permeability analyses predict the excess pore pressure dissipation process better. For analysis 6 (varied II), the soil elements under the embankment yielded at an early stage of construction (OCR=1.2) and after yielding, the soil permeability was varied with the initial value of low permeability (Table 1). However, the soil elements away from the embankment may not yield in the whole construction process, and thus, still possess with high value of permeability. The overall effect is that the predicted excess pore pressures are higher than those obtained using middle permeability (Table 1) at end of construction and closer to the value of using middle permeability at later stages of consolidation.

Settlements

The predicted and measured surface settlements under the center point of reinforced mass are compared in Fig. 8. The locations of settlement plate is also shown by the key sketch in the figure. It can be seen that the predicted values have remarkable agreement with measured data. However, the varied permeability analyses yielded higher settlement rate at the early stage of construction and lower settlement rate during the consolidation process.

The settlement profile on the cross-sectional lines on the ground surface is plotted in Fig. 9. The comparisons are given for both immediately after construction and one year after construction conditions. From the figure, it can be seen that the agreement between the predicted and measured data are reasonably good. Unfortunately, there are no measured data for foundation heave. The predicted maximum foundation heave infront of the wall face is 125 mm immediately after construction. One year after construction, it reduced to 62 mm. As mentioned previously, the varied permeability analysis (varied II) allows the variation of the permeability in the horizontal direction with high value for the soil elements away from the embankment loading area, and the subsequent predicted value of heave is less than that of the constant permeability analysis. For example, at end of construction, the maximum heave is 110 mm. This tendency seems more closer to field behavior, since most finite element analyses using constant permeability overpredicted the foundation heave (e.g. Magnan and Kattan, 1989).

Lateral Displacements

Lateral displacement is one of the most difficult items to predict. Figure 10 is the comparison of predicted and measured lateral displacement profiles for both end of construction and 7 months after construction cases. For lateral displacements in the foundation soils, the measured data up to 7 months after construction only reach down to 3 m depth because the inclinometer probe could not be inserted into the deformed casing below 3 m depth. At the end of construction, the predicted wall face lateral displacements agreed well with the measured data. However, the predicted subsoil lateral displacements are twice as large as that of measured data. At 7 months after construction, the predicted subsoil and wall face lateral displacements reasonably agreed with the measured values. However, at the top of the wall face, the predicted values are less than the measured ones and the predicted maximum subsoil lateral displacements are still larger than the field data. It also can be seen that compaction effect increased wall face lateral displacement by about 10% at end of construction even with the light compactor. This effect became less significant at one year after construction.

The time-lateral displacement relationship is shown in Fig. 11 for two points, namely: (a) top of the wall face and (b) 3 m below the original ground surface where maximum lateral displacement occurred in the foundation. For the top of the wall face, the discrepancy between the predicted and the measured values appears at 3 months after the construction (August 20, 1989). At that time the measured data showed an increased rate of lateral displacements, it was probably due to the occurrence of heavy rainfall because there was a sudden ground water level increase at that time (Bergado et al, 1991). For the point under the wall face and 3 m below original ground surface, the discrepancy between the predicted and the measured lateral displacements mostly occurred during the construction period. After construction, both the predicted and the measured lateral displacements show small increment rate. There are two reasons for the differences obtained between the measured lateral displacements and those predicted by the finite element analyses, namely: (1) the deficiency of the analytical method (Poulos, 1972); and (2) the influence of inclinometer casing stiffness which may result in relative displacements between the soil and the casing because it is difficult for casing to freely follow the "S" shape deformation pattern (see Fig. 10).

Tension Forces in Reinforcements

The predicted maximum tension forces in reinforcements at immediately after construction and one year after construction are shown in Fig. 12, together with the measured data at immediately after construction. Also shown are the active and at-rest earth pressure lines without considering the cohesion in drawing the active earth pressure line. The agreement between predicted and field data for immediately after construction case is quite good. The data are presented in terms of per meter width and per reinforcement layer (0.45 m). The measured data one year after construction was not included because of too much scatter. Both the predicted and measured data

showed that at the end of construction, the maximum tension forces in the reinforcements at the top half of the wall are much larger than k_o line. At the middle wall height, the data are closer to the k_o line. At the bottom of the wall, the data are much higher than k_o line again. For reinforced wall on soft ground, under the wall loading, the soft soil tends to squeeze out of the wall/embankment base which causes large relative movement between the reinforcement and the soil. Therefore, large tension force can be developed in the reinforcements. The maximum tension forces in the reinforcements increased during the foundation soil consolidation process. At the top half of the wall, the maximum reinforcement tension forces after one year of construction are twice as large as those immediately after construction due to the large lateral displacement of the wall face. The figure also shows that the compaction effect may cause the tension force in reinforcement at the top of the wall increase significantly.

The tension force distributions along the reinforcements for instrumented mats are shown in Fig. 13. Generally speaking, the agreement between the predicted and measured data for immediate after construction case is fair. The reinforcement tension force distribution pattern was strongly influenced by the interaction between the reinforced wall/embankment mass and soft foundation soil. The foundation differential settlement cause the bending effect on the reinforced mass, i.e. top in compression and bottom in tension. So that the length of the reinforcement in tension is short in upper part of the wall. The figure also shows that the location of maximum tension force is very close to the wall face (less than 1.0 m) except at the base reinforcement layer.

Wall/Embankment Base Pressures

The base pressure is an important item for design of reinforced wall and embankment on soft ground because it controls the safety factor of bearing capacity of the foundation. Figure 14 shows the predicted and measured total earth pressures at the base of the reinforced mass. The comparison is not very good, but it is qualitatively sufficient. From vertical force equilibrium point of view, the measured data was relatively low even considering the stress spreading due to the foundation settlement. Nevertheless, there are two points that can be made from the predicted total base pressure distribution. Firstly, the predicted earth pressure distribution is more likely trapezoidal pattern, even though there is a stress concentration under the wall face. Secondly, during the foundation consolidation process, there is a reduction in the total base pressure, and an increase in stress concentration under the wall face. This is because of during the foundation consolidation process, the reinforced mass sinks into the ground, and the vertical load is distributed into a larger horizontal area. At the same time, the overturning movement of the reinforced mass also increased due to the differential settlement. The overall effect is the increased stress concentration under the wall face and the reduction of the base pressure at other locations.

DIFFICULTIES IN PREDICTION

Difficulties Related to Determine the Input Parameters

As mentioned previously, the correctness of finite element results depends largely on both the constitutive model and the value of model parameters used. Although most of the model parameters can be determined from high quality laboratory test results with confidence, some parameters, such as soft soil permeability, are very difficult to determine. The laboratory permeability test can be subjected to error resulting from the size of sample, temperature, and the large difference between the hydraulic gradient in the field and in the laboratory. For Bangkok clay, as reported by Bergado et al (1990), the laboratory test values underestimated the field permeability significantly. Field permeability measurements such as the piezometer method can be affected by the clogging of the filters and disturbance of the soil during the equipment installation.

The values derived from back analysis of existing case histories are of great help for determining the actual permeability values. For Bangkok clay, the values of field permeability are about 10 to 30 times of the corresponding laboratory test data. Another point is the variation of the permeability. This factor has been noticed long time back (e.g. Taylor, 1948). In order to precisely predict the behavior of the embankment on soft ground, it is necessary to consider the variation of the permeability with the yielding and the change the void ratio of the soil.

Difficulties in Modelling

The stress/strain behavior of the soil is influenced by several factors, such as elasto-plastic behavior, nonhomogeniety, anisotropy, and structure of the soil, the stress path followed by the soil, etc. Even the sophisticated soil model, such as the modified Camclay model cannot consider all these factors. At present, the settlement can be predicted reasonably well, but the agreement between predicted and measured lateral displacements is fair to poor. This phenomenon had been discussed by Poulos (1972) who cited such reasons as: the effect of Poisson's ratio, anisotropy, and nonhomogeniety which appeared to be most significant factors. Normally, the maximum lateral displacement occurs at the vicinity of the embankment toe, where considerable principal stress rotation occurs during the embankment construction. Most of the above mentioned factors cannot be properly modelled and some of them are still not well understood, such as the effect of the principal stress rotation on the behavior of soil.

CONCLUSIONS

The finite element modelling techniques presented in this paper improved the ability of finite element method to predict the behavior of the reinforced earth structure on soft ground. The modelling demonstrates that the soil/reinforcement interaction

properties can be properly selected according to the relative displacement pattern between soil and reinforcement (direct shear or pullout), and the construction process can be most closely simulated.

Comparing the predicted and measured data indicates that the performance of the reinforced embankment on soft ground can be predicted by finite element method by selecting the foundation permeability based on back analyzed values from case histories and by considering the compaction effect on the embankment fill. It has been found that the predicted foundation settlements and wall face lateral displacements agreed reasonably well with the field data, and the agreement between predicted excess pore pressures, tension force in reinforcements, foundation lateral displacements, and embankment base pressures is fair. It was also observed that using constant permeability cannot precisely simulate the excess pore pressure variation. Regarding the discrepancy between the predicted and measured foundation lateral displacement, two reasons are cited as follows: (1) the deficiency of the analytical method, and (2) the measured data might be influenced by inclinometer casing stiffness.

REFERENCES

Adib, M.Mitchell, J.K. and Christopher, B. (1990), Finite element modelling of reinforced soil walls and embankments, design and performance of earth retaining structure, ASCE Geotech. Special Publication, No.25, 409-423.

Ahmed, M.M. (1977). "Determination of permeability profile of soft Rangsit clay by field and laboratory tests". M. Engrg. Thesis, No. 1002, Asian Institute of Technology, Bangkok, Thailand.

Asakami, H. (1989). "The smear effect of vertical band drains". M. Engrg. Thesis, No. GT-88-8, Asian Institute of Technology, Bangkok, Thailand.

Balasubramaniam, A.S., Hwang, Z.M., Vddin, W., Chaudhry, A.R. and Li, Y.G. (1978). "Critical state parameters and peak stress envelopes for Bangkok clays". Q. J. Engrg. Geol., 11, 219-232.

Bergado, D.T., Sampaco, C.L., Alfaro, M.C., and Balasubramaniam, A.S. (1988). "Welded-wire reinforced earth (mechanically stabilized embankments) with cohesive backfill on soft clay". Second Progress Report Submitted to USAID Bangkok Agency.

Bergado, D.T., Ahmed, S., Sampaco, C.L., and Balasubramaniam, A.S. (1990). "Settlements of Bangna-Bangpakong Highway on soft Bangkok clay, J. of Geotech. Engrg. Div., ASCE, 116(1), 136-155.

Biot, M.A. (1941), General Theory of Three-Dimensional Consolidation, J. Of Applied Physics, 12, 155-164.

Britto, A.M. and Gunn, M.J. (1987). Critical state soil mechanics via finite elements, Ellis Horwood.

Chai, J.C. (1992). "Interaction behavior between grid reinforcement and cohesive-frictional soil and performance of reinforced wall/embankment on soft ground". D. Engrg. Dissertation, Asian Institute of Technology, Bangkok, Thailand.

Clough, G.W. and Duncan, J.M. (1971). "Finite element analysis of retaining wall behavior". J. of Soil Mech. and Found. Engrg. Div., ASCE, 97(12), 1657-1673.

Collin, J.G. (1986). "Earth wall design". Ph.D. Thesis, Univ. of California, Berkeley.

Duncan, J.M., Byrne, P., Wong, K.S. and Mabry, P. (1980). "Strength, stress-strain and bulk modulus parameters for finite element analysis of stresses and movements in soil". Geotech. Engrg. Research Report No. UCB/GT/80-01, Dept. of Civil Engrg., Univ. of California, Berkeley, August, 1980.

Duncan, J.M. and Seed, R.B. (1986). "Compaction-induced earth pressure under K_o-condition". J. of Geotech. Engrg. Div., ASCE, 112(1), 1-22.

Hird, C.C. and Pyrah, I.C. (1990). Predictions of the behavior of a reinforced embankment on soft ground, Proc. Symp. on Performance of Reinforced Soil Structures, Thomas Telford, 409-414.

Lambe, T.W. (1973). Predictions in soil engineering (Rankine Lecture), Geotechnique, 23(2), 149-202

Macatol, K.C. (1990). "Interaction of lateritic backfill and steel grid reinforcements at high vertical stress using pullout test". M. Engrg. Thesis, GT-89-12, Asian Institute of Technology, Bangkok, Thailand.

Magnan, Jean-Pierre and Kattan, A. (1989). Additional analysis and comments on the performance of Muar flats trial embankment to failure. Procedings of the Int. Symp. on Trial Embankments on Malaysian Marine Clays, Vol. 2, 11/1-11/7.

Poulos, H.G. (1972). "Difficulties in prediction of horizontal deformations in foundations." J. of Soil Mech. and Found. Engrg. Div., ASCE, 98(8), 843-848.

Roscoe, K.H. and Burland, J.B. (1968). "On the generalized stress-strain behavior of wet clays". Proc. of Engrg. Plasticity, Cambridge, Cambridge Univ. Press, 535-609.

Rowe, R.K. and Mylleville, B.L.J. (1988). " The Analysis of steel reinforced embankment on soft clay foundation". 6th Int. Conf. on Numerical Methods in Geotechnics, Innsbruck, 1273-1278.

Shivashankar, R. (1991). "Behavior of a mechanically stabilized earth (MSE) embankment with poor quality backfills on soft clay deposits, including a study of the pullout resistances". D. Engrg. Dissertation, Asian Institute of Technology, Bangkok, Thailand.

Tavenas, F. & Leroueil, S. (1980), The behavior of embankments on clay foundations, Can. Geotech. J. 17, 236-260.

Tavenas, F., Jean, p., Leblond, P., and Leroueid, S. (1983). "The permeability of natural soft clays, part II, permeability characteristics." Can. Geotech. J. 20, 645-660.

Taylor, D.W. (1948). Fundamentals of soil mechanics. John Wiley & Sons Inc. New York.

Table 1. Soil Parameters of Bangkok Clay

Parameter	Soil Layer						
	Symbol		1	2	3	4	5
	Depth, (m)		0-1	1-2	2-6	6-8	8-12
Kappa	κ			0.04	0.11	0.07	0.04
Lambda	λ			0.18	0.51	0.31	0.18
Slope	M			1.1	0.9	0.95	1.1
Gamma (P'=1 kPa)	Γ			3.0	5.12	4.0	2.9
Poisson's Ratio	ν		0.25	0.25	0.30	0.30	0.25
Modulus, (kPa)	E		4000				
Friction Angle, (°)	ϕ'		29.0				
Cohesion, (kPa)	C'		29.0				
Unit Weight, (kN/m^3)	γ		17.5	17.5	15	16.5	17.5
Horizontal Permeability (m/sec), (10^{-8})	High	k_h	69.4	69.4	10.4	10.4	69.4
	Middle	k_h	34.7	34.7	5.2	5.2	34.7
	Low	k_h	13.9	13.9	2.1	2.1	13.9
Vertical Permeability (m/sec), (10^{-8})	High	k_v	34.7	34.7	5.2	5.2	34.7
	Middle	k_v	17.4	17.4	2.6	2.6	17.4
	Low	k_v	6.9	6.9	1.0	1.0	6.9

NOTE: High: k_v = 50 times of estimated average test value;
Middle: k_v = 25 times of estimated average test value;
Low: k_v = 10 times of estimated average test value.
Horizontal permeability is always 2 times of the vertical value.

Table 2. Hyperbolic Soil Parameters Used for Lateritic Backfill Material

Para-meter	Cohesion C, (kPa)	Friction Angle ϕ, (°)	Modulus Number k	Modulus Exponent n	Failure Ratio R_f	Bulk Modulus Number k_b	Bulk Modulus Exponent m	Unit Weight γ,(kN/m^3)
Value	60	32.5	1078	0.24	0.96	1050	0.24	20.0

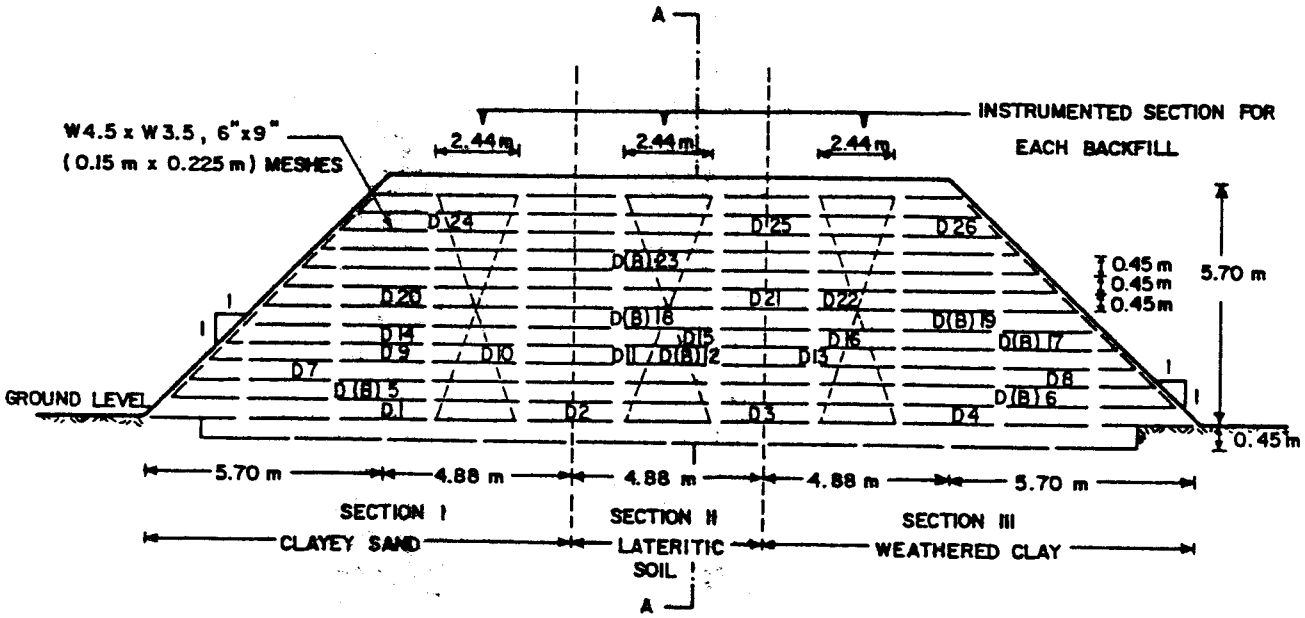

(a) Longitudinal-Section View

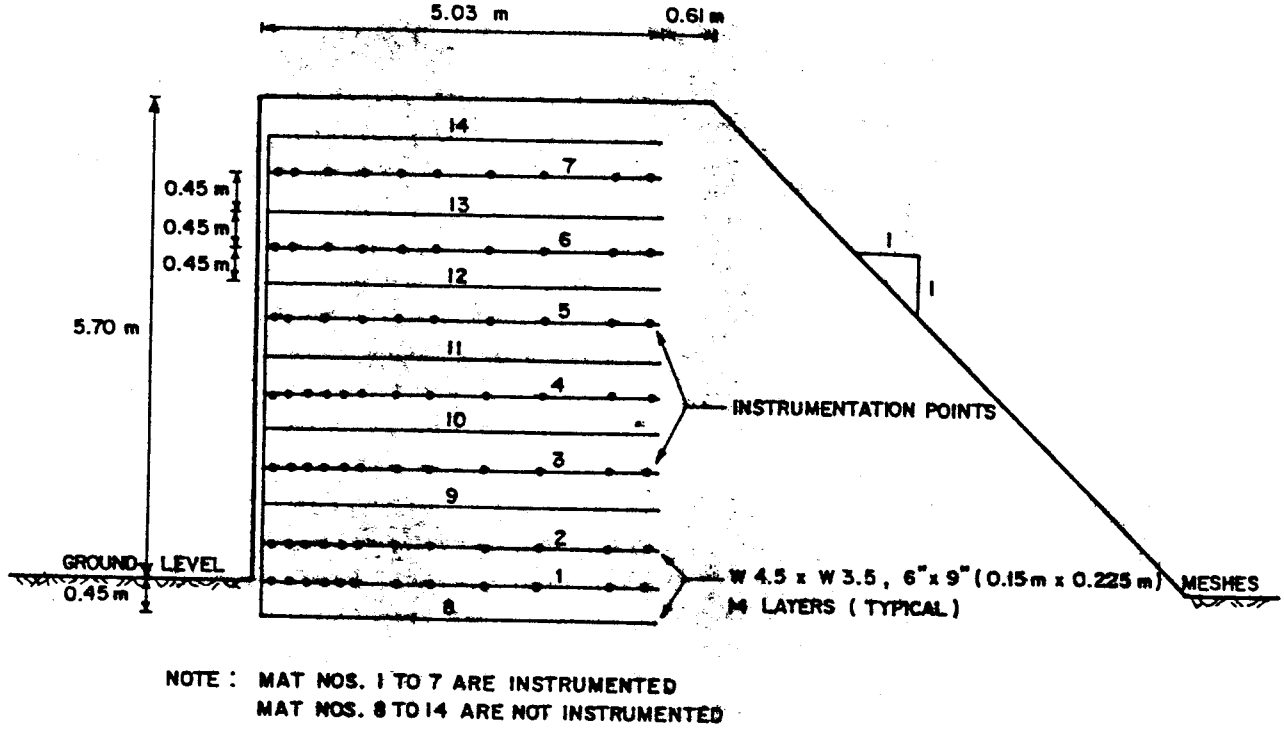

(b) Cross-Section View

Fig. 1 Cross-sectional view of the test reinforced wall/embankment

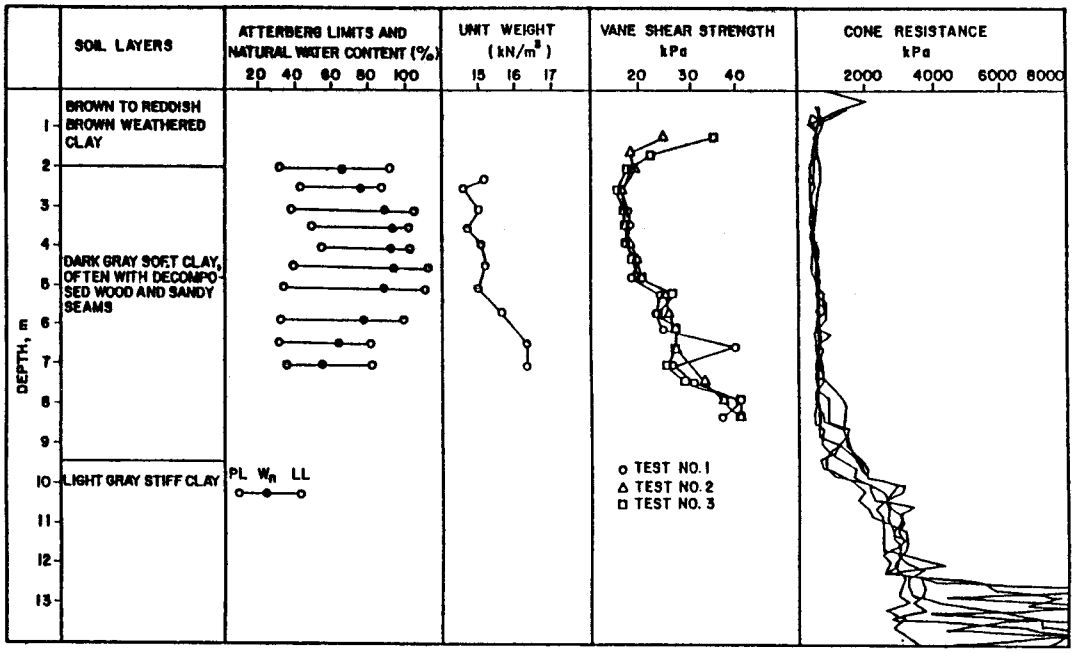

Fig. 2 Index properties, vane shear strengths and Dutch cone resistances of the subsoil at test site

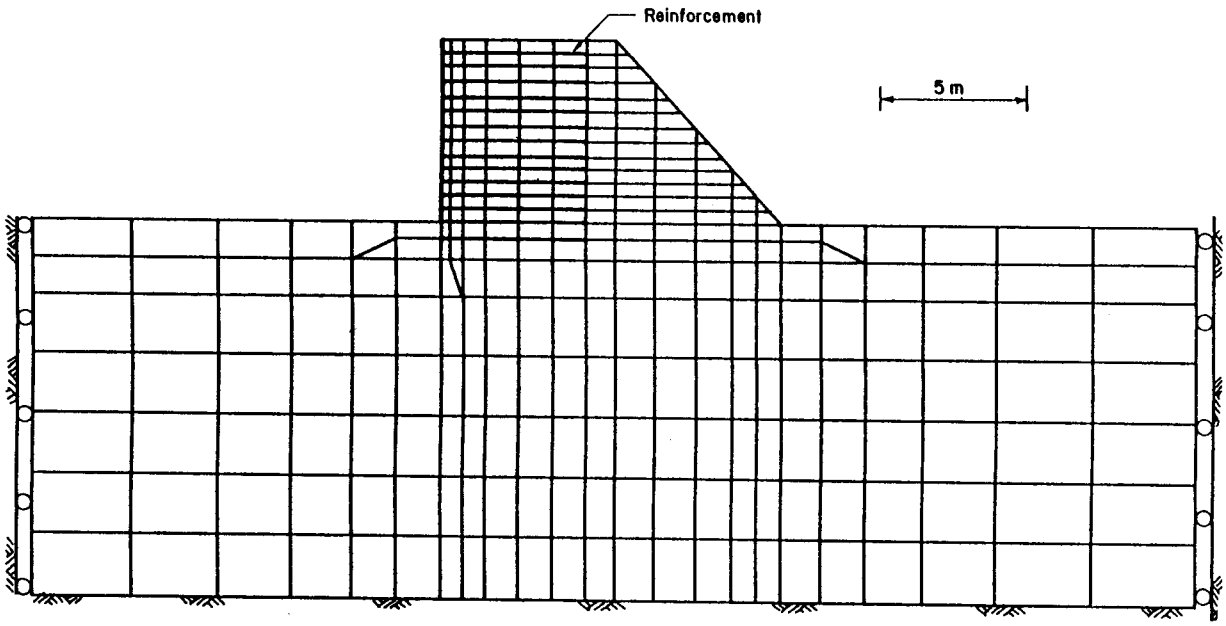

Fig. 3. Finite element mesh used for AIT test reinforced wall/embankment

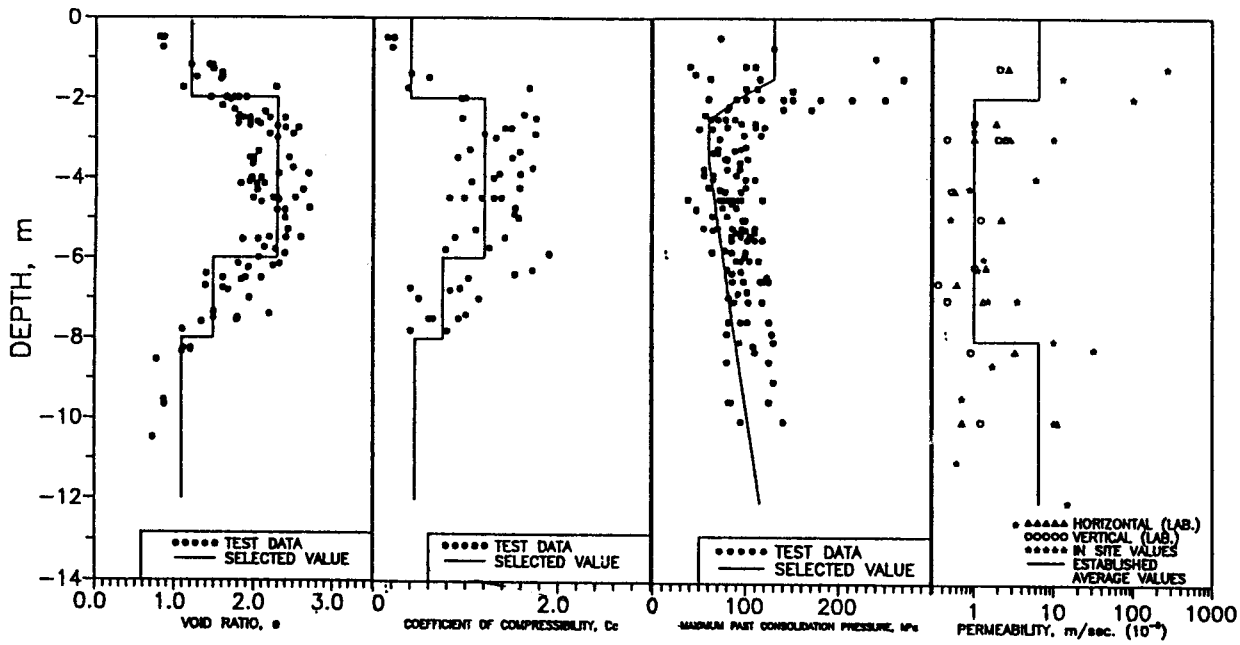

Fig.4. Void ratio, compressibility index, past maximum vertical pressure, and laboratory permeability of the Bangkok clay

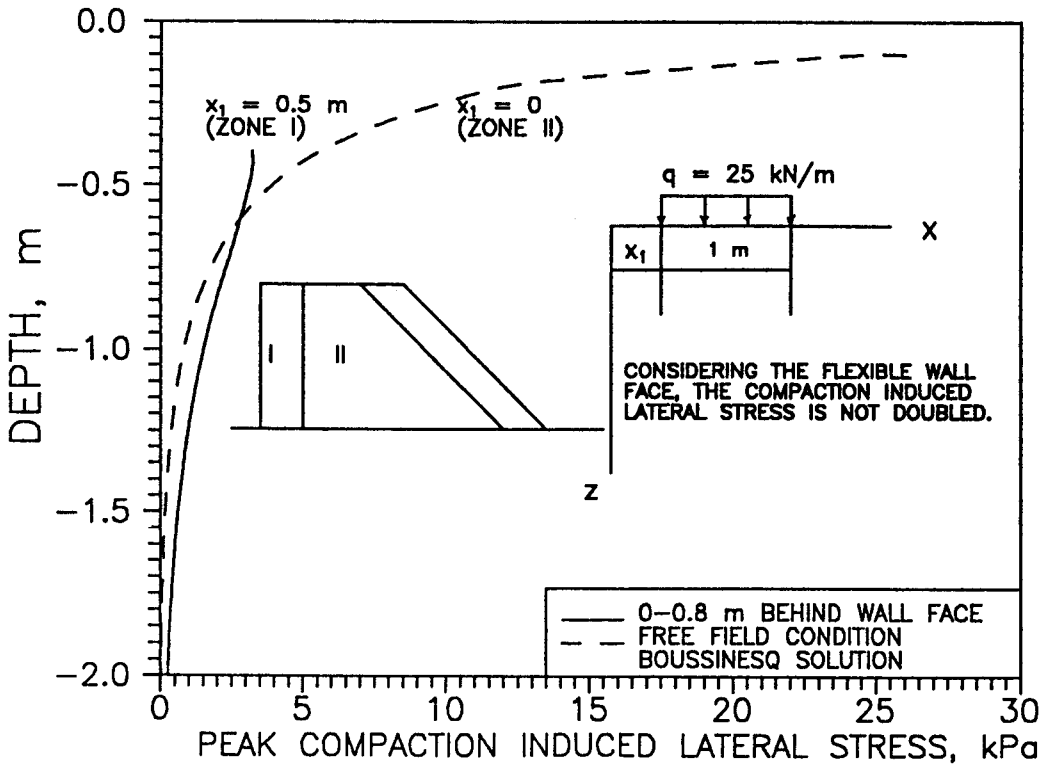

Fig. 5. Maximum compaction induced lateral earth pressures

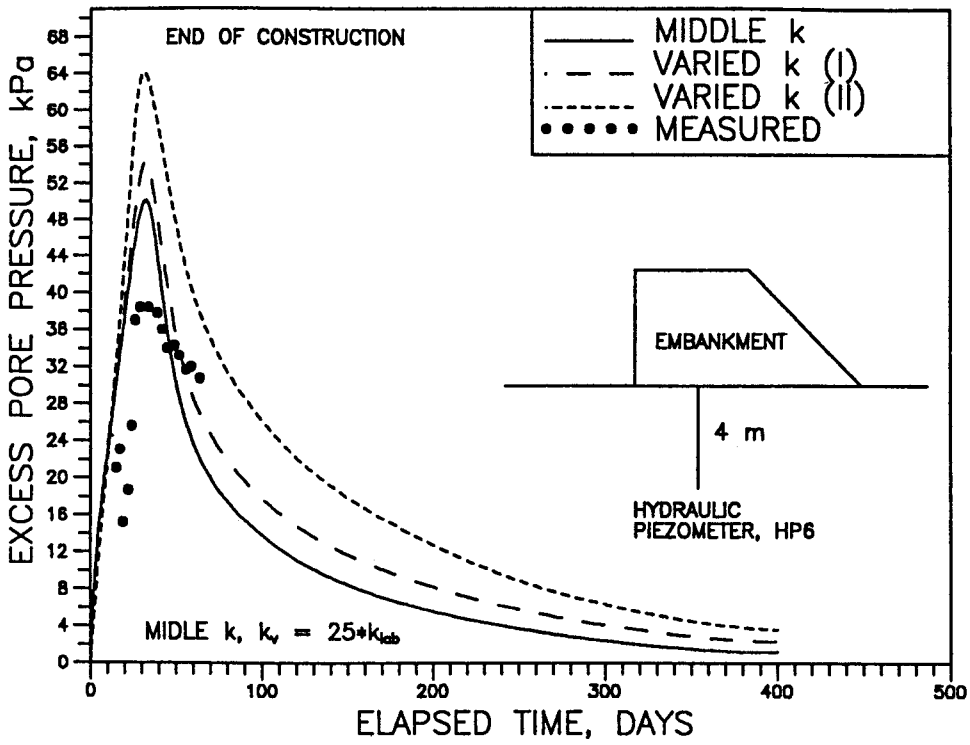

Fig. 6. Predicted and measured excess pore pressure variation at piezometer point HP6

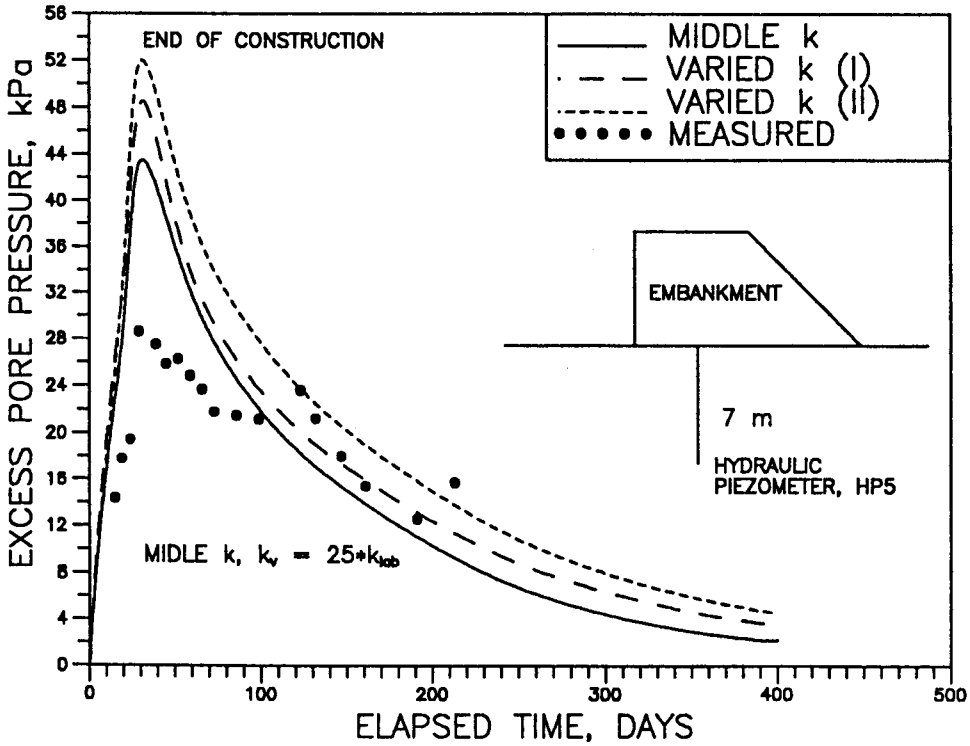

Fig. 7. Predicted and measured excess pore pressure variation at piezometer point HP5

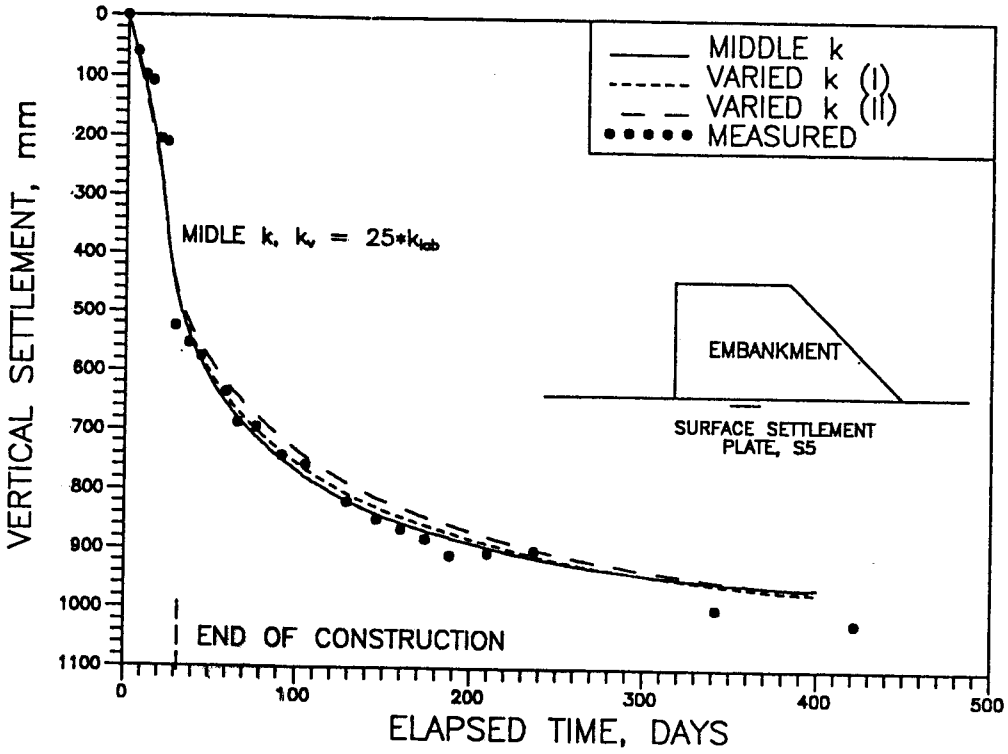

Fig. 8. Typical predicted and measured settlement curves

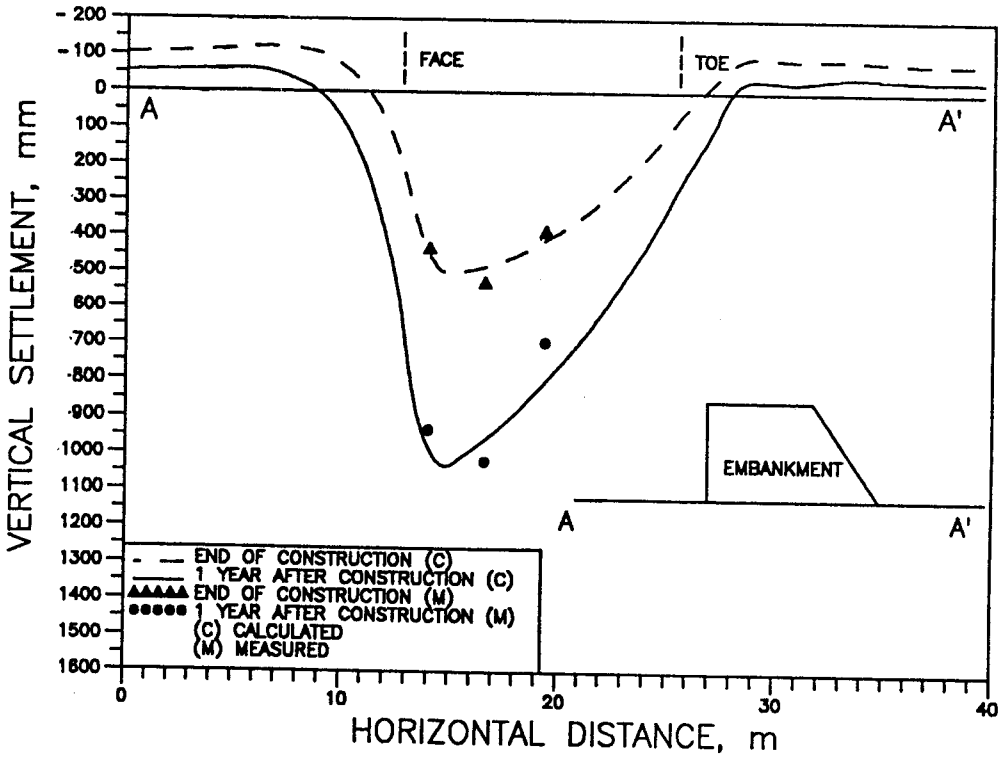

Fig. 9. Predicted and measured surface settlement profiles

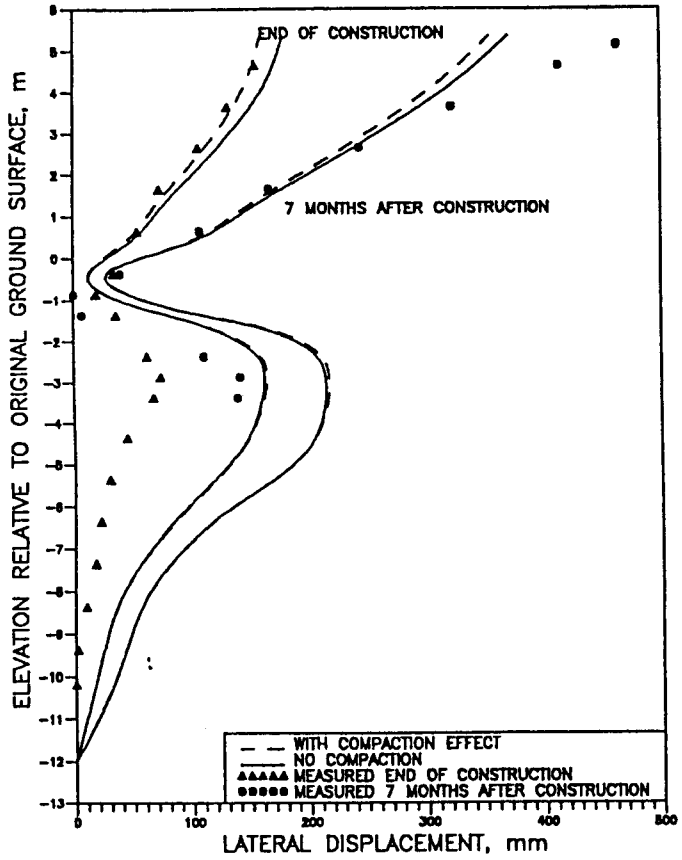

Fig. 10. Lateral displacement profiles

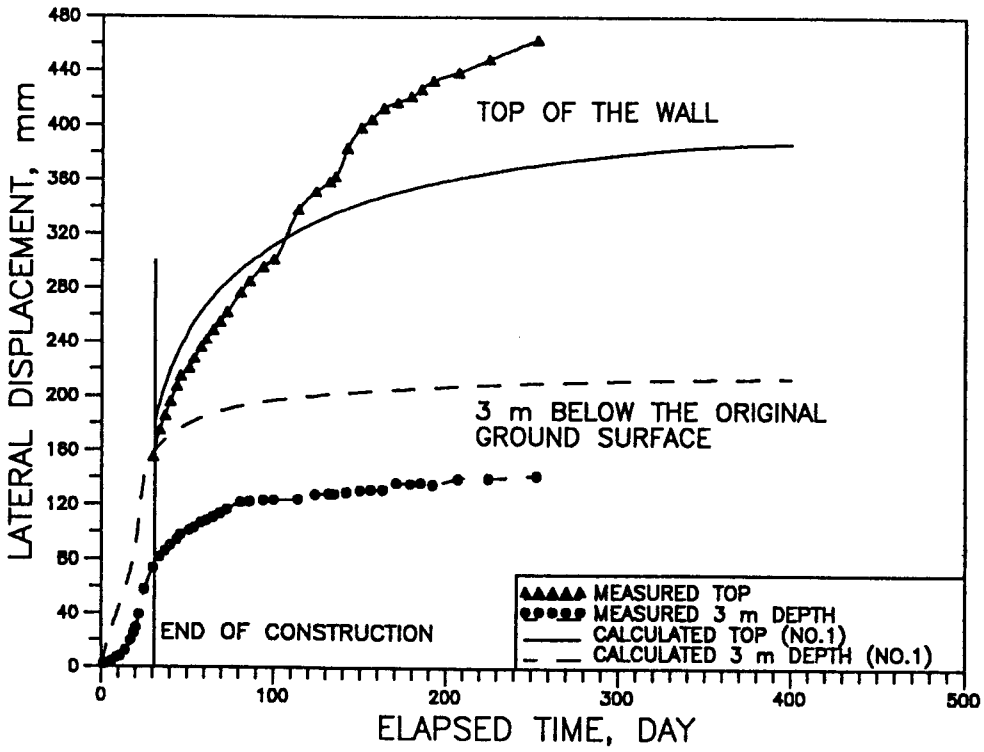

Fig. 11. Maximum lateral displacement curves

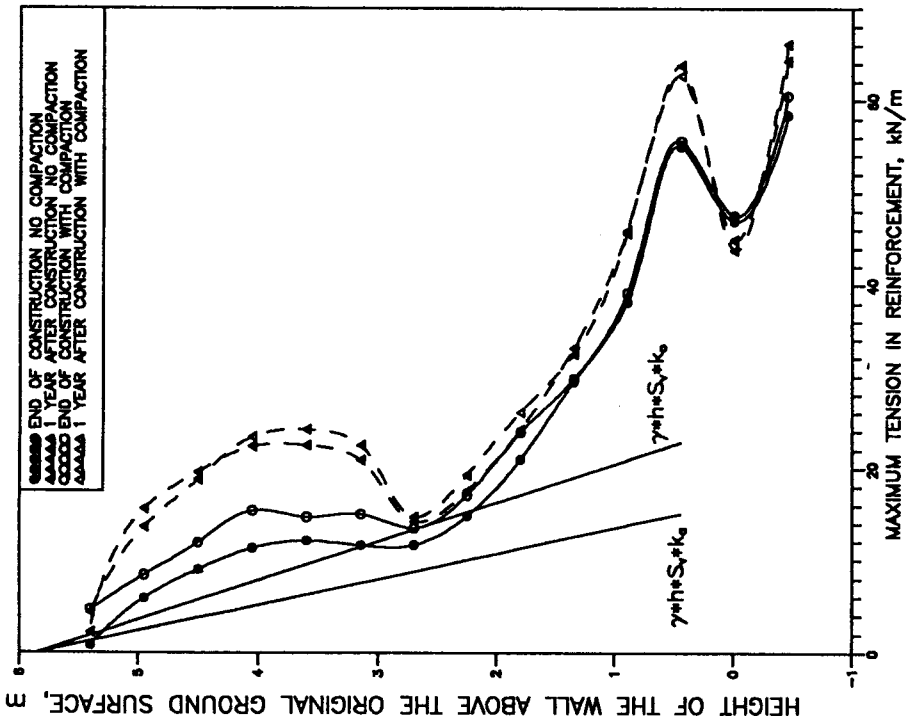

Fig. 12. Maximum reinforcement tension force profiles

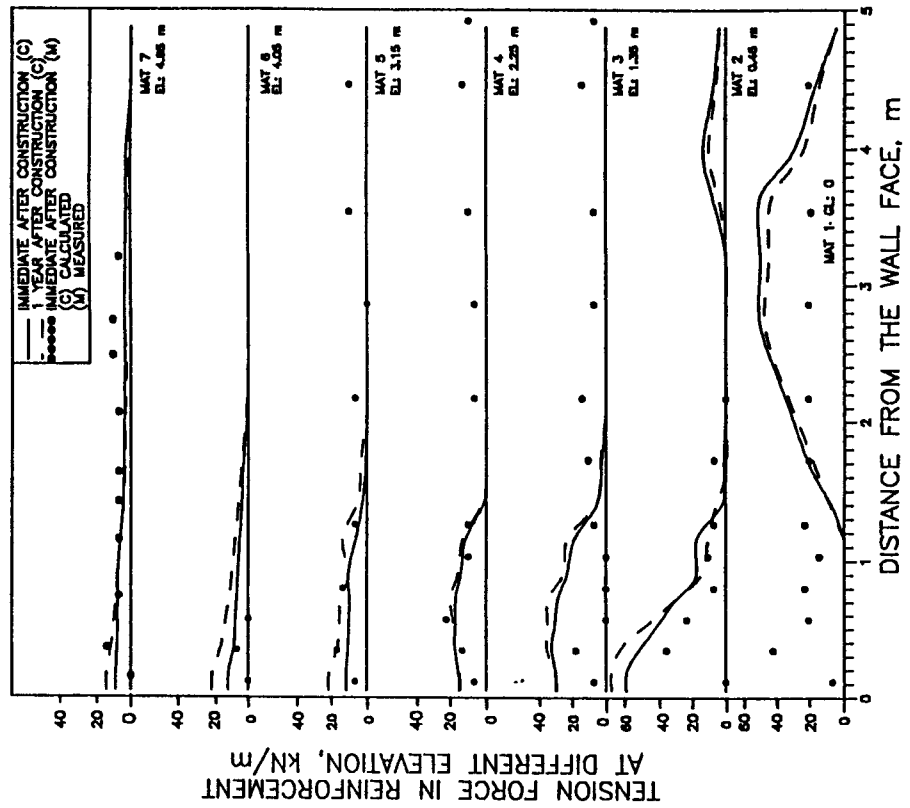

Fig. 13. Reinforcement tension force distributions

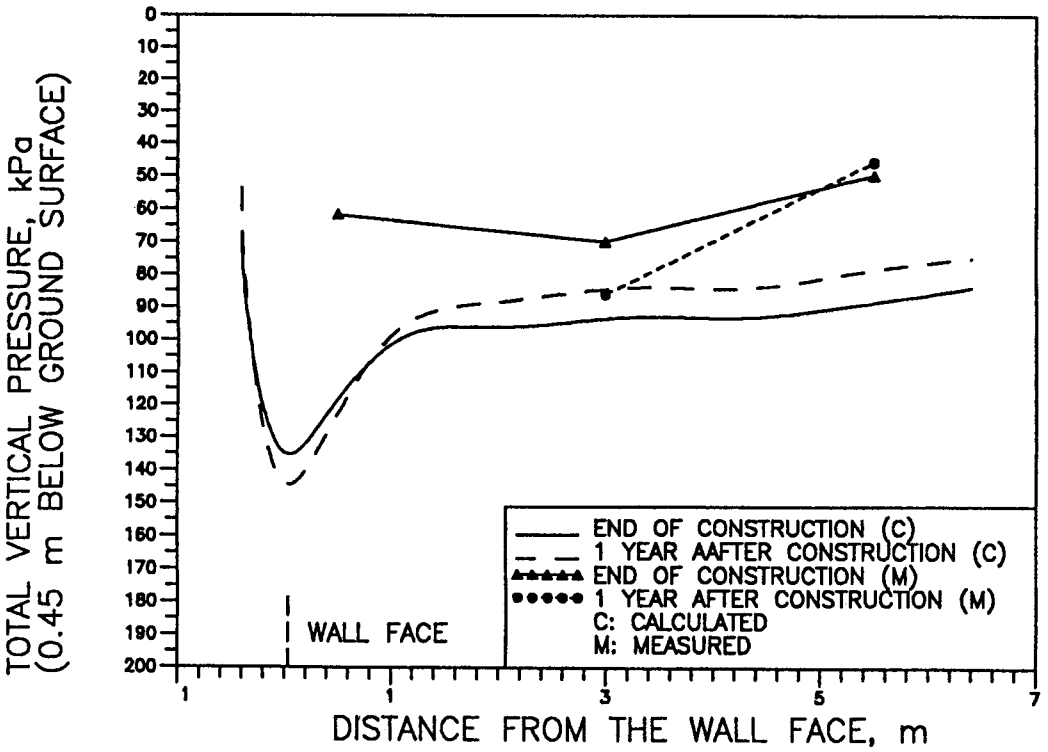

Fig. 14. Predicted and measured total embankment base pressure